

Potential of INSAT-3D Sounder Derived Total Precipitable Water Product for Weather Forecast

Shailesh Parihar*, A.K. Mitra, M. Mohapatra and ^aR. Bhatla

India Meteorological Department, New Delhi-110003

^a*Banaras Hindu University, Varanasi-221005*

*Email- shellsalpha@gmail.com

Abstract

The objectives of the INSAT-3D satellite are to enhance the meteorological observations and to monitor the Earth surface for weather forecasting and disaster warning. One of the weather monitoring capability in the INSAT-3D sounder is the estimation of water vapor in the atmosphere. The amount of the water vapor present in the atmospheric column is derived as the total precipitable water (TPW) product from the infrared radiances measured by INSAT-3D sounder. The improvement in the estimation of TPW is carried out by applying the GSICS calibration corrections (Global Space-based Inter-Calibration System) to the radiances from Infra-Red (IR) channels of the sounder, which is done using IMDPS (INSAT Meteorological Data Processing System). The present study is based on TPW derived from INSAT-3D sounder, Radiosonde (RS) observations and corresponding to National Oceanic and Atmospheric Administration (NOAA) satellite. To assess retrieval performances of INSAT-3D sounder derived TPW, RS TPW observations are considered for the validation during May to September 2016 from 34 stations of India Meteorological Department (IMD) is considered for the validation. The analysis is performed on daily, monthly and sub-divisional basis over the Indian region. The comparison of INSAT-3D TPW with RS TPW on daily and monthly basis shows that the root mean square error (RMSE) and correlation coefficients (CC) are ~8 mm and 0.8, respectively. However, on sub-divisional and overall scale, the RMSE found to be in the range of 1 to 2 mm and CC was around 0.9 in comparison with RS and NOAA. The spatial distribution of INSAT-3D TPW with actual rainfall observation is also been investigated. In general, INSAT-3D TPW correspond well with rainfall observation however, heavy rainfall events occurs in the presence of high TPW values. In addition, utilizing the TPW from INSAT-3D and ground based Global Navigation Satellite System (GNSS) receiver network, the case studies of thunderstorm events shows good agreement during the

31 mesoscale activity. The current TPW from INSAT-3D satellite can be utilized operationally for
32 weather monitoring and forecast purpose and it can also offer substantial opportunities for
33 improvement in nowcasting studies.

34 **Keywords:** INSAT-3D Sounder, Total Precipitable Water, rain fall.

35

36

1. INTRODUCTION

37 Water vapour is one of the most variable quantities in the troposphere, playing a crucial role in the
38 climate and weather. It regulates air temperature by absorbing thermal radiation both from the sun
39 and the Earth; it is directly proportional to the latent energy available for the generation of storms;
40 and it is the ultimate source of all forms of condensation and precipitation. Latent heat released
41 during cloud formation cloud dominate the structure of diabatic heating of the atmosphere
42 (Trenberth et al., 2005; Trenberth and Stepaniak, 2003a, b). The observations of Total Precipitable
43 Water (TPW) are essential for weather and climate modeling and prediction. The TPW may be
44 used for monitoring the mesoscale to synoptic scale convective activity, monsoonal activities, and
45 moisture gradients. It have shown the significant improvement in precipitation forecasts when
46 TPW is incorporated in the numerical weather prediction models (Kuo et al., 1996). Utilizing the
47 TPW data, (Yuan et al. 1993) showed ~8 mm increment in the tropical TPW resulting from
48 doubling of atmospheric CO₂. The water vapor varies in time and as well as in space (both
49 vertically and horizontally) and the gaps in the observations makes its use impossible for climate
50 and weather forecasting/nowcasting related studies (Trenberth and Olson, 1988). This could be
51 possible with higher temporal and spatial resolution of accurate temperature and moisture profile
52 either from in-situ observations or remotely sensed data. Recently, The Sounder for Atmospheric
53 Profiles of Humidity in the Inter-tropical Regions (SAPHIR) on board Megha-Tropiques satellite
54 has made the RH profiles available in the tropical latitudes (Ratnam et al., 2013). SAPHIR has
55 good spatial coverage with limited temporal resolution.

56 The products, especially the retrievals of vertical profiles of temperature and humidity, from the
57 sounder of INSAT-3D satellite are important in weather monitoring and forecasting as well as in
58 the study of mesoscale weather phenomena. The higher ground resolution of 10 km and high
59 vertical resolution (about 1 km) along with hourly observations from INSAT-3D sounder provides
60 frequent information on the 3D structure of atmospheric temperature and humidity for the whole
61 Earth disk seen by the satellite (except in and below clouds). They could be used together with the

62 imagers, to produce high resolution cloud detection or water vapor features, to track rapidly
63 evolving phenomena. However, the INSAT-3D sounder observations of TPW are limited for sky
64 conditions (Ratnam et. al., 2016).

65 In the present study, the TPW derived from INSAT-3D sounder is statistically compared with
66 radiosonde observations and NOAA satellite data over the period May to September 2016. The
67 purpose of this comparison is to investigate the potential of operational hourly TPW product for
68 the monitoring of weather phenomenon over the Indian region. However, initial work using
69 INSAT-3D sounder data was carried out by Mitra et al. 2015, showing the comparison of INSAT-
70 3D data with RS observations from 10 stations of IMD (India Meteorological Department).
71 Utilizing the RS observations from 34 stations and data from ERA-Interim, NCEP re-analysis
72 and other satellites like AIRS, MLS, SAPHIR, Ratnam et al. 2016 showed the reasonable
73 agreement among these datasets. It is shown that there is a large difference between INSAT-3D
74 and other data sets; both in temperature and water vapour above 25 °N latitude; perhaps due
75 to difference in their geometries (Ratnam et al., 2016). In the present paper, we extend the work
76 with 34 RS stations and taking NOAA data on daily, monthly, sub divisional scale followed by
77 case studies with IMD installed network of GNSS TPW. Furthermore, the spatial distribution of
78 INSAT-3D TPW with actual rainfall observation has also been investigated.

79

80

2. DATASETS

2.1 INSAT-3D Sounder Scan Processing Strategy

2.1.1 INSAT-3D Sounder Specification

83 INSAT-3D is advance weather satellite with improved imaging system and atmospheric sounding.
84 The observations of INSAT-3D sounder are utilized to retrieve the vertical profile of the
85 atmosphere in terms of temperature and humidity. INSAT-3D sounder has one visible spectral
86 channel and eighteen channels in shortwave infrared (SWIR), middle infrared (MIR) and long
87 wave infrared (LIR) regions. For all the channels, the ground resolution is 10×10 km. The further
88 detail of INSAT-3D sounder can be found elsewhere (Mitra et.al, 2015).

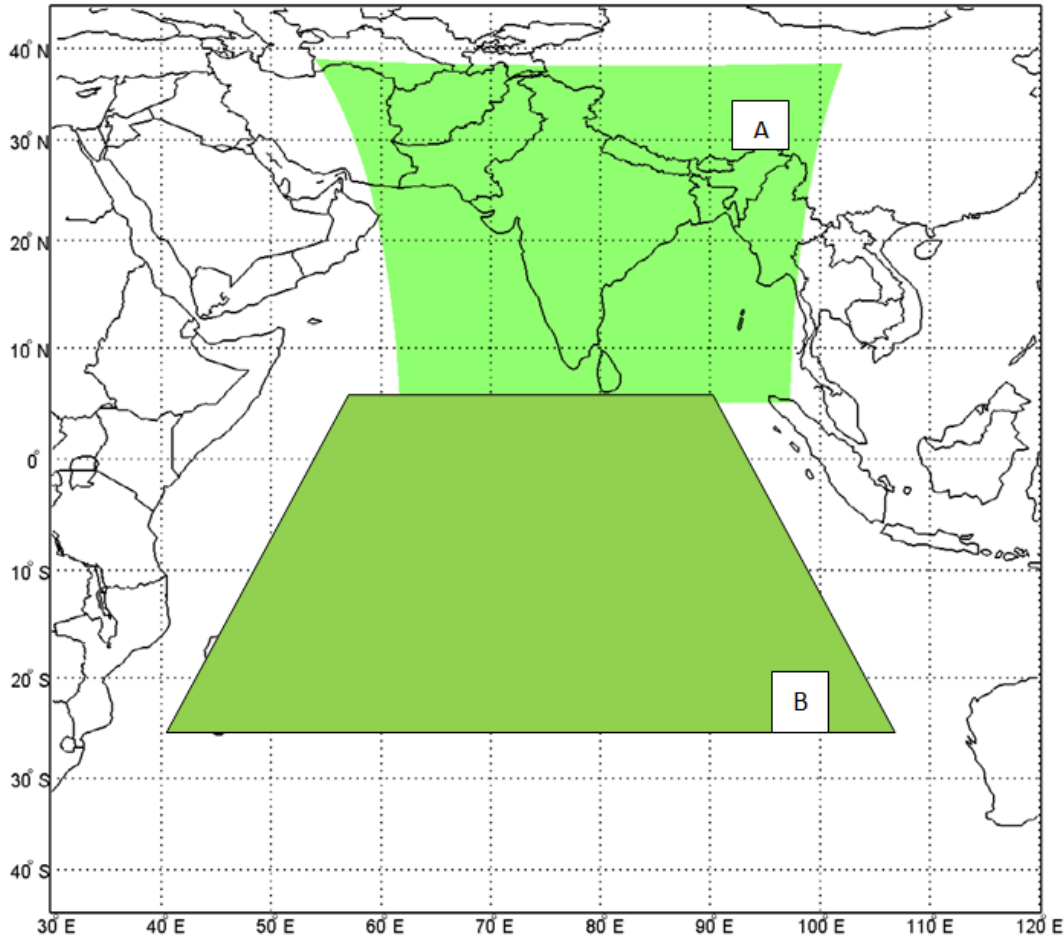
89

Table 1 Sounder Specification

Channels (Spectral Range Microns)	Resolution
Visible (0.67)	10X10 Km
SWIR (3.67)	10X10 Km
MIR (6.38)	10X10 Km
LWIR (11.66)	10X10 Km

90 *2.1.2 INSAT-3D Sounder Scan Processing Strategy*

91 INSAT-3D scans in the full frame mode which is $18^{\circ} \times 18^{\circ}$ North South (NS) covering the entire
92 Earth disc in about 25.7 minutes. Figure 1 shows the areas over Indian land mass (A) and over the
93 southern hemisphere (B) over which the sounder data is being processed by IMDPS
94 (Meteorological Data Processing System), New Delhi on an operational basis. While the Indian
95 land mass is scanned at every hour interval, it is 6 hour interval for the southern hemispheric area.
96 This is the simple scanning strategy kept in such a way that sounding over larger region
97 (land+ocean) will be available every hour. Sounder completes sounding in $10 \text{ km} \times 10 \text{ km}$ area in
98 0.1 second and performs space look operation once every 2 minutes. Black body calibration is
99 performed in every 20 minutes or on command basis. INSAT-3D Sounder have a capability to
100 scan in the steps of 64×64 pixels. Scanning of a region covering 640×640 pixels that is roughly
101 $6400 \text{ km} \times 6400 \text{ km}$ takes ~ 180 minutes. The benefit of this kind of scan strategy can be utilize
102 for the studies of initial convections, genesis of evolution of squall lines and their fine structures
103 (Purdom et al., 1996a). The INSAT-3D sounder scan strategy can be used for nowcasting and
104 NWP (Numerical Weather Prediction) model assimilation over Indian region.



105

106

Figure 1. INSAT-3D Sounder scan processing strategy over land and ocean.

107

2.2 Radiosonde Observations (RS)

108

In IMD, upper air observations are made at 43 RS stations, 34 RS stations are being used and 62

109

Pilot Balloon observatories to provide pressure, temperature, humidity & wind at various levels in

110

the atmosphere up to an altitude of 30-35 km. **Figure 2 shows the location (marked in red color)**

111

of 34 RS stations. Observations from these stations are utilised for the comparison with INSAT-

112

3D TPW. The types of ground equipment used in RS observatories are (1) Radiosonde Ground

113

equipment (ECIL/DIGITAL make) along with X band Win, (2) d finding Radars

114

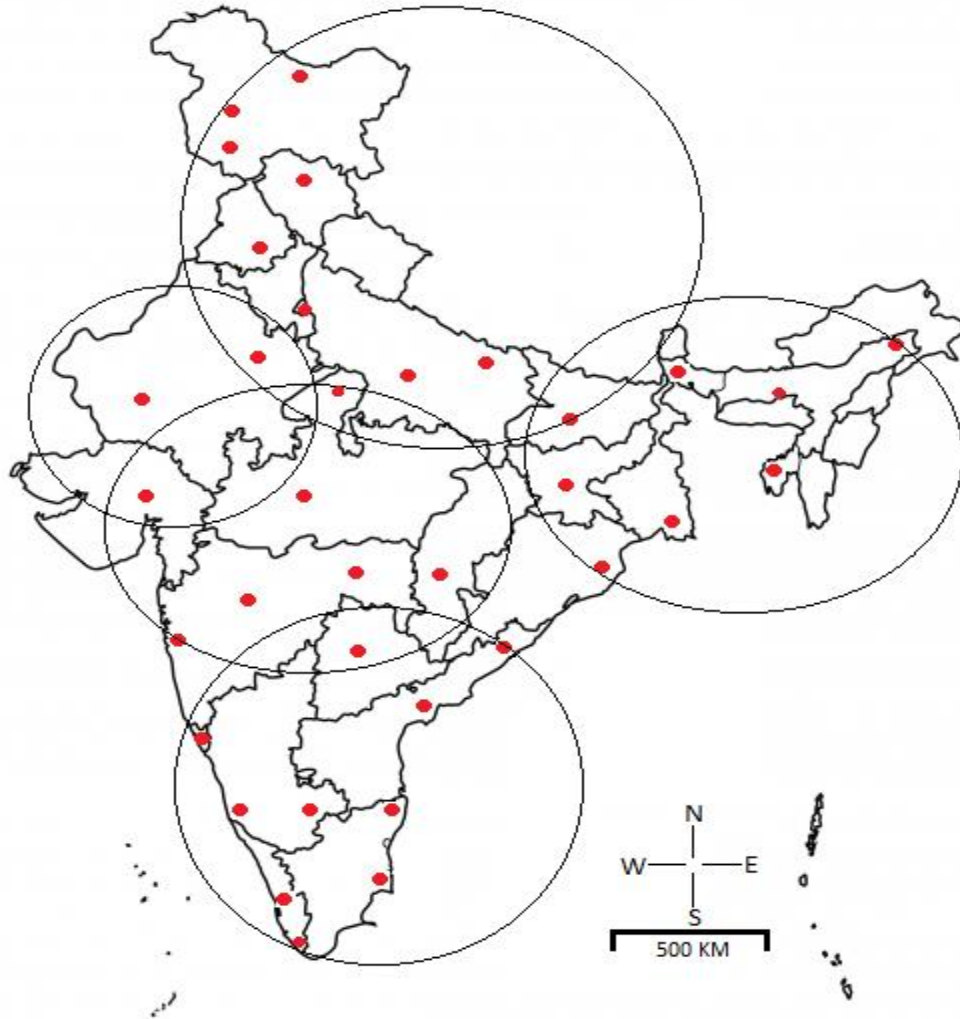
(EEC/MULTIMET) at 401 MHz and (3) IMS-1500 Radiotheodolite at 1680 MHz and SAMEER

115

Radiotheodolite at 401 MHz. The performance of IMD's GPS radiosonde stations has been very

116

well examined using ECMWF global data (Gajendra Kumar et al., 2011).



117

118 **Figure 2. Radiosonde Stations (red dots) of IMD over India. Areas marked with ellipses**
 119 **represent different sub-divisions.**

120 **2.3 Global Navigation Satellite System (GNSS)**

121 IMD is augmenting Integrated Network of Global Navigation Satellite System (GNSS) receivers
 122 from 5 to 30 for integrated precipitable water vapour (IPWV) measurements. The network is
 123 capable of using other GNSS Network data of research institutes in real time basis for enhancing
 124 data spatial density and processing. The equipment has advanced meteorological sensors to
 125 measure temperature, pressure, humidity of the station and capable of working independently in
 126 all-weather condition with high temporal resolution. **Though satellites don't often fail, if one fails**

127 **GNSS receivers can pick up signals from other satellites of the system. The data can be found from**

128 <http://gnss.imd.gov.in/>.

129 **2.4 NOAA's satellite observation**

130 The NOAA (National Oceanic and Atmospheric Administration) Satellite and Information Service
131 provides timely access to global environmental data from satellites and other sources to monitor
132 and understand the atmospheric variation over the Earth in efficient manner. In this study, we used
133 blending TPW from two satellite sources, one from the Advanced Microwave Sounding Unit
134 (AMSU) instruments on NOAA satellites (Ferraro et al., 2005), and the other from the Special
135 Sensor Microwave Imager (SSM/I) instruments on Defence Meteorological Satellite Program
136 (DMSP) satellites. In the blended Total Precipitable Water (TPW) product, individual biases of
137 the data sources have been mitigated to produce a more meteorologically significant product.
138 Blending retrieval procedure has detailed (Kidder et al., 2007) and methodology provides seamless
139 global coverage without gaps to allow for the analysis of atmospheric moisture over land and ocean
140 (Schmit et al., 2002 and Smith et al., 2007). The products are on a Mercator projection with 16 km
141 resolution at the equator. The products are hourly in HDF-EOS file format. These operational
142 products were produced by the NOAA/NESDIS (National Environmental Satellite, Data, and
143 Information Service) Office of Satellite and Product Operations (OSPO).

144 **2.5 GSICS based inter-calibration**

145 There is an on-board blackbody which is responsible for generation of calibration information
146 for all the IR channels in the sounder. In-orbit readings of blackbody
147 temperatures revealed a gradient among the sensor which led to inaccuracy in getting
148 the correct blackbody temperature. It was also observed that during satellite midnight, sun-rays
149 from behind the Earth enter directly into the sensor and hence lead to increase in blackbody
150 temperatures. This phenomenon leads to generation of incorrect calibration information. In order
151 to provide climate quality products and to improve the calibration coefficients, GSICS (Global
152 Space based Inter calibration System) based inter-calibration is used for INSAT-3D. The GSICS
153 aims to inter-calibrate a diverse range of satellite instruments, to produce corrections ensuring
154 consistency in satellite dataset. Allowing usage of calibration data, it produces globally
155 homogeneous products for environmental monitoring. In addition, GSICS develops common
156 methodologies to check the quality of sensors operated by various satellite agencies over the
157 worldwide. The post launch calibration strategy involves spectral response function of sensors,

158 sensor performances and inter-calibration of satellite sensor. And finally, recalibration of archived
159 data or products of sensors is carried out, if necessary. The channel wise GSICS coefficient are
160 found and applied in during the Radiometric Correction process.

161

162

3. METHODOLOGY

163 INSAT-3D retrieval algorithm under IMDPS at New Delhi, is designed for retrieving vertical
164 profiles of atmospheric temperature and moisture from clear sky infrared radiances measured over
165 different absorption bands (<http://www.imd.gov.in/INSAT-3D/categouge>). The observed radiance
166 in various sounder channels are processed on an hourly time scale. IMD, New Delhi has adapted
167 sounder retrieval scheme from the operational High resolution Infrared Radiation Sounder (HIRS)
168 processing scheme and Geostationary Operational Environmental Satellites (GOES) algorithms
169 developed by Cooperative Institute for Meteorological Satellite Studies (CIMSS), University of
170 Wisconsin, USA (Ma et al., 1999 and Li et al., 2000). In this scheme, physical and regression
171 based retrievals are employed, which includes spectral bands in and around the CO₂ and H₂O
172 absorbing bands. In the scheme, computation of the hybrid first guess atmospheric profiles is using
173 linear combination of regression retrieval and NWP model forecast (Mitra et al., 2015). The
174 methodology has followed by non-linear physical retrieval procedure (Li et al., 2000 and Ma et
175 al., 1999) for the consistency with the sounder observations. The Pressure layer Fast Algorithm
176 for Atmospheric Transmittance (PFAAST) radiative transfer model (Hanon et al., 1996) has been
177 used for forward computation of sounder channel radiances along with Jacobians. As mentioned
178 before, GSICS corrections have been incorporated in the INSAT-3D sounder radiances.

179 Mathematically, if a(p) is the mixing ratio at the pressure level, p, then the precipitable water vapor
180 W, contained in a layer bounded by pressures p₁ and p₂ is given by

181
$$\text{INSAT3D Precipitable Water Vapor} = \frac{1}{\rho g} \int_{p_1}^{p_2} a dp$$

182 Where ρ represents the density of water and g is the gravity constant (9.8 m/s²). Further details can
183 be found at <http://www.imd.gov.in/INSAT-3D/categouge>.

184 The each RS observation was paired with closest INSAT-3D TPW and patterned according to
185 criteria suggested in Fuelberg and Olson (1991).The collocation criteria for INSAT-3D retrievals

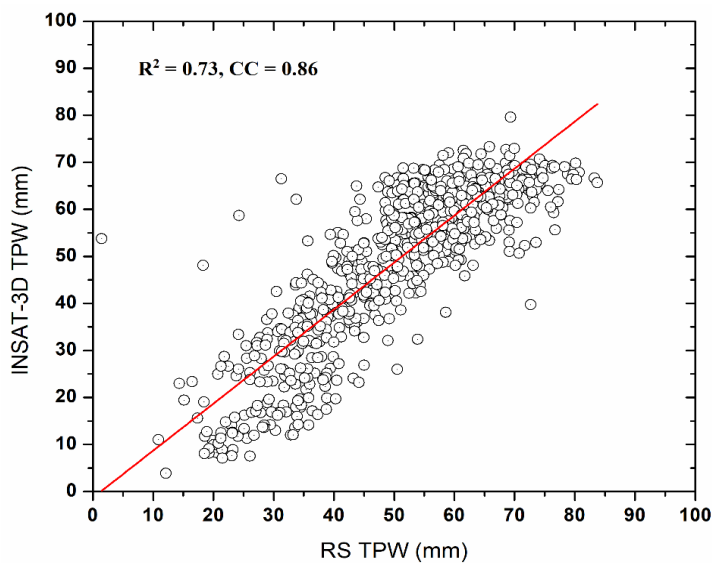
186 with RS and NOAA data are based on the following. (1) The absolute distance between the position
187 (latitude and longitude) of the RS and the INSAT-3D retrievals is 0.5° (50 Km) or smaller. This
188 will minimize the differences arising from horizontal gradients in water vapor or TPW. (2) The
189 temporal difference between two sets of data is around ± 120 minutes depending on retrievals and
190 location of the RS station. (3) The timing of INSAT-3D and RS observations was matched at 0000
191 and 1200 UTC.

192

193 4. RESULTS AND DISCUSSIONS

194 4.1 Comparison of INSAT-3D with RS and NOAA TPW at Daily, Monthly and Sub Division 195 Scales

196 INSAT-3D derived TPW is available at hourly interval over the Indian region. For validation
197 purposes of TPW and its usefulness in weather monitoring and forecast, it is desirable to compare
198 INSAT-3D TPW at different time scales with different sets of data. Thus, on a daily scale, we
199 compared the INSAT-3D TPW with all the collocated measurements of RS TPW. On monthly
200 scale, monthly averaged data on collocated points were used. For sub-division scale, five different
201 regions categorized according to meteorological subdivisions are, Northern India (NI), Eastern
202 India (EI), Central India (CI), Western India (WI) and Peninsular India (PS) (Figure 2).

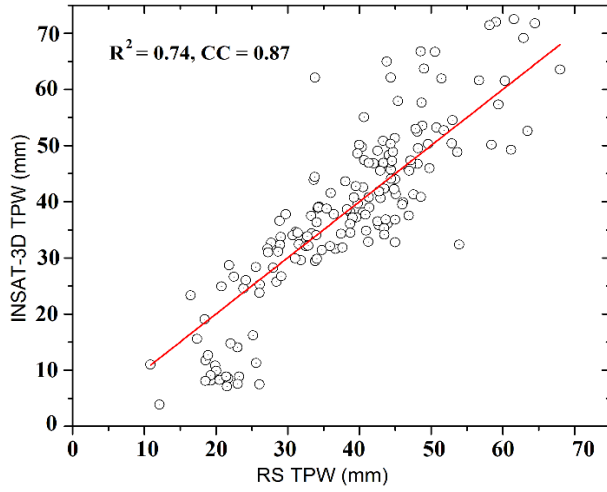


203

204 **Figure 3. Comparison of INSAT-3D derived TPW with RS observed TPW from May to**
205 **September 2016**

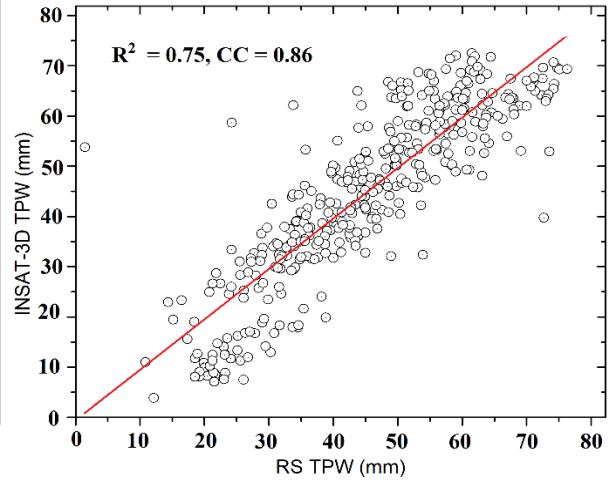
206 Figure 3 shows the comparison of INSAT-3D TPW and RS TPW on daily scale during May-
207 September 2016. On day to day basis, INSAT-3D TPW agrees well with RS TPW. INSAT-3D
208 TPW is able to measure the synoptic features of weather phenomena at monthly scale over the
209 Indian region very well. However magnitude differs, it can be termed as source of error due to
210 registration and navigation issues during the night time. The consistent and better correlation has
211 seen above 40 mm of TPW values, whereas for less than 40 mm TPW values, INSAT-3D
212 underestimates slightly. This is due attributed to seasonal variation, orographic of the region and
213 different climatic zone over India. The largest differences are observed mainly over mountainous
214 areas and/or near the sea, which reveal differences in representativeness. Good confidence in
215 INSAT-3D TPW estimates is gained during periods of moderate to heavy rain. The overall
216 correlation on daily scale was found to be 0.86. In the previous study, (Mitra et al., 2015) reported
217 0.73 correlations using 10 IMD stations.

218 Figure 4 shows the comparison of INSAT-3D TPW and RS TPW on Monthly scale during May-
219 September 2016. The correlation coefficients are in the range of 0.78-0.87. It can be noticed that
220 during monsoon period, specially in the month of June, July and August, when heavy rainfall
221 (above 64.5 mm) occurs, INSAT-3D TPW shows well agreement with RS TPW. Mostly INSAT-
222 3D TPW is higher when rainfall occurrence is higher above 40 mm. The statistics corresponding
223 to this comparison is shown in table 2. INSAT-3D coefficients of variation are high as compared
224 with RS, which indicates the higher variability in total precipitable water. The mean difference
225 between RS and INSAT-3D TPW is much higher in the month of July 5.57 mm. It is due to the
226 substantial rainfall during the monsoon season and in the subsequent months August and
227 September 5.24, 5.3 mm respectively. It was also reported by (Ratnam et al., 2016) that mean
228 difference in the water vapor is as high as 20-30%. The dry basis of 10-25% in INSAT-3D channel
229 compare to similar satellite and reanalysis dataset was also noted. The coefficient of variation is
230 lower for the months July to September, 2016. The coefficient of skewness found negative between
231 INSAT-3D and RS measurement, which indicates mean is less than the mode of the data. The
232 correlation coefficient show good agreement with RMSE for June to September, 2016 except in
233 the month of July. The student's t-test calculated for significance of computed parameter. The
234 student's t-test shows the statistical significance of linear relationship among the data, i.e. INSAT-
235 3D TPW and RS TPW.



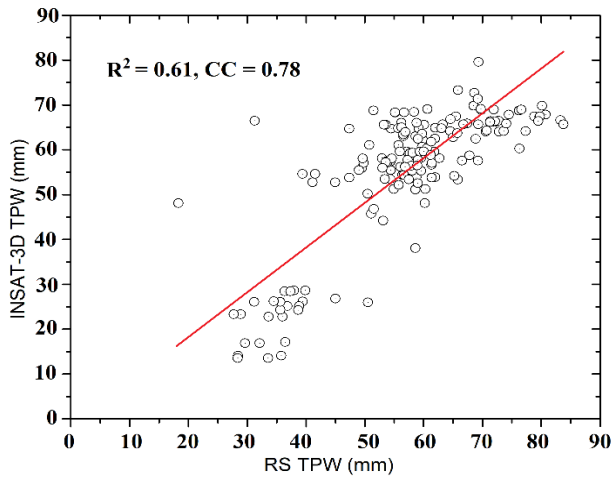
236

May



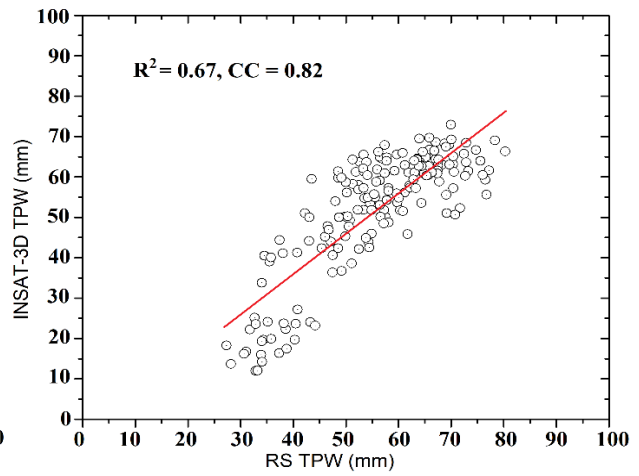
237

June



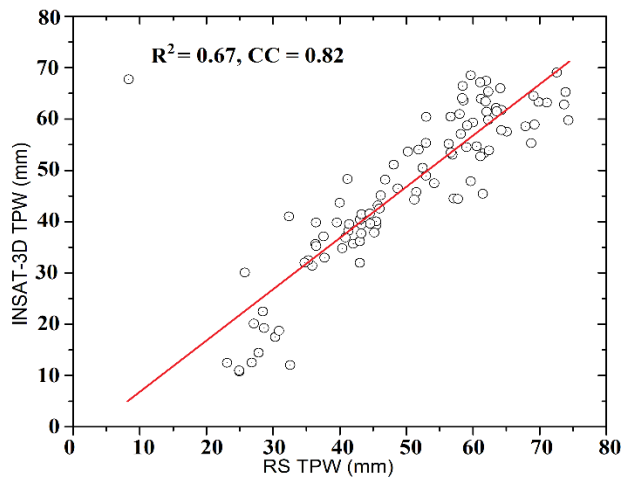
238

July



239

August



240

September

241

242 **Figure 4. INSAT-3D sounder TPW with RS for May, June, July, August and September**
 243 **2016**

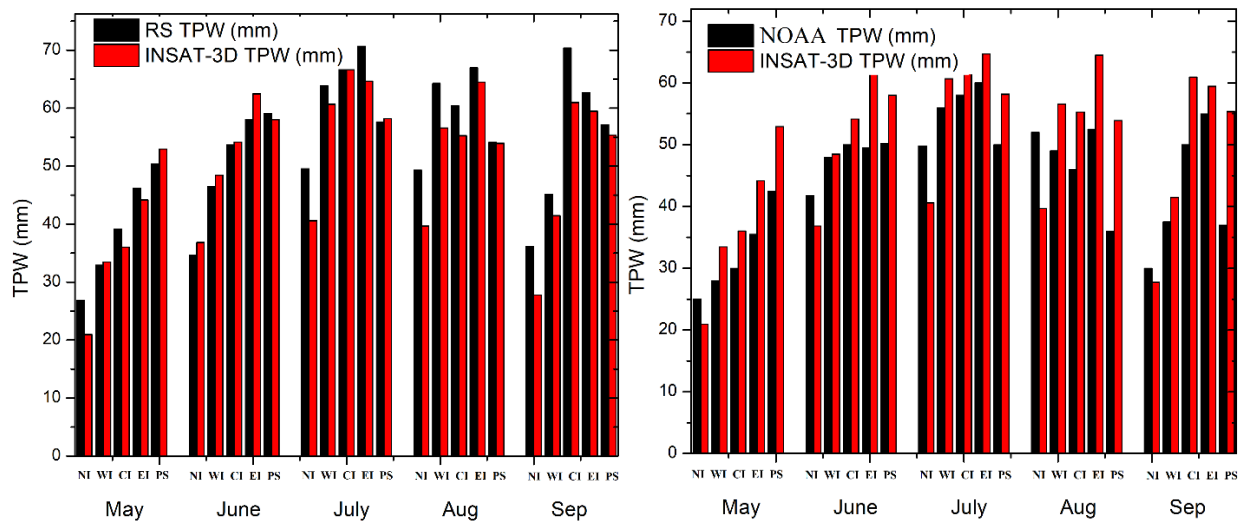
244 **Table 2. Statistics and correlation between total precipitable water measured by INSAT-3D**
 245 **and RS**

Mo nth	INSAT -3D	RS	INSAT -3D	RS	INSAT -3D	RS	INSA T-3D	RS	CC	RMSE (mm)	t-test
	Arithmetic Mean (mm)		Standard Deviation		Coefficient of Variation		Coefficient of Skewness				
May	39.36	39.87	15.40	12.51	0.39	0.31	-0.21	-0.10	0.87	7.69	0.359931
Jun	49.75	52.66	16.44	14.16	0.33	0.26	-0.87	-0.57	0.86	8.50	0.049282
July	54.87	60.44	14.59	12.53	0.26	0.20	-1.45	-0.61	0.78	9.31	0.000012
Aug	52.09	57.33	14.71	11.97	0.28	0.20	-1.24	-0.49	0.82	8.73	0.000022
Sep	49.00	54.30	14.14	13.69	0.28	0.25	-1.01	-0.31	0.82	8.79	0.000213

246
 247 Figure 5 shows the comparison of INSAT-3D TPW with RS TPW and NOAA TPW on sub
 248 divisional scale during May to September 2016. It can be clearly seen from the figures that INSAT-
 249 3D TPW is underestimating whereas it is over estimating the NOAA TPW for the entire region
 250 during the monsoon period. A good correlation is observed for the region, CI and PS as compared
 251 to EI and NI regions. However, opposite trend were found while comparing INSAT-3D TPW with
 252 NOAA TPW. INSAT-3D TPW is always higher over NOAA data. One of the possible reasons is
 253 that INSAT-3D sounder derived TPW were calculated from the radiances sampled every hour
 254 while NOAA TPW were based on only two satellite passes with equator crossing times of 0230
 255 and 1430 local time (in Indian Standard Time). Therefore, the sampling frequency of the
 256 radiometer is much higher in a geostationary satellite than polar satellite. In general, sub-divisional
 257 comparison reveals that the INSAT-3D TPW agrees well RS and NOAA TPW below 23° N
 258 whereas the difference is higher above 23°N.

259 The table 3 shows the statistics for the comparison of TPWs from INSAT-3D, RS and NOAA at
 260 the subdivisions in India. INSAT-3D coefficients of variation are similar to that of RS, but in case
 261 of NOAA it is higher with respect to INSAT-3D and RS. The coefficient of skewness values found

262 negative for INSAT-3D, RS and NOAA measurement. The correlation coefficients how good
 263 agreement between INSAT-3D and NOAA (0.96) as well as between INSAT-3D and RS (0.87)
 264 during June to September, 2016.
 265



266
 267 **Figure 5. Comparison of INSAT-3D derived with RS and NOAA observed TPW sub-**
 268 **division scales NI, WI, CI, WI & PS from May to September 2016**

269 **Table 3. Statistics of INSAT-3D derived, RS and NOAA observed TPW sub-division**
 270 **scales of India**

Sub div.	Sensors	Arithetic Mean	SD	Coefficient of Variation	Coefficient of Skewness	NOAA vs INSAT-3D			INSAT-3D vs RS		
						BIAS	RMSE	CC	BIAS	RMS E	CC
NI	NOAA	39.71	11.91	0.30	-0.29	1.3	1.09	0.97	1.22	1.15	0.87
	INSAT-3D	33.16	8.51	0.25	-0.84						
	RS	39.28	9.91	0.25	0.005						
WI	NOAA	43.7	10.98	0.25	-0.63	-0.88	0.88	0.97	0.47	0.77	0.97
	INSAT-3D	48.13	11.04	0.22	-0.26						
	RS	50.52	13.42	0.26	-0.12						
CI	NOAA	46.8	10.35	0.22	-1.22	-1.56	1.23	0.97	0.79	0.83	0.96
	INSAT-3D	54.61	11.51	0.21	-1.20						
	RS	58.58	12.83	0.21	-0.90						
EI	NOAA	50.5	9.22	0.18	-1.28	-1.71	1.27	0.91	0.37	0.83	0.91
	INSAT-3D	59.05	8.58	0.14	-1.92						

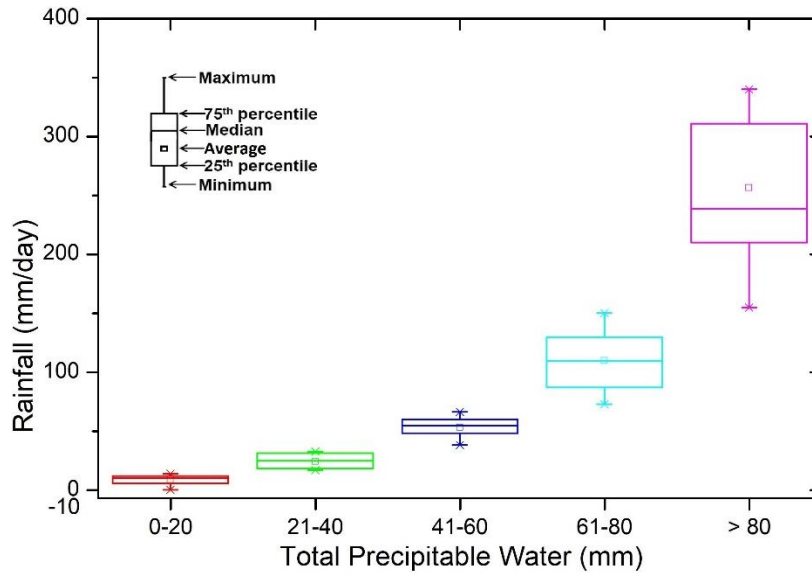
	RS	60.92	9.47	0.15	-1.00							
PS	NOAA	43.14	6.81	0.15	0.10	-2.5	1.55	0.77	-	0.002	0.45	0.92
	INSAT-3D	55.68	2.36	0.04	0.05							
	RS	55.66	3.44	0.06	-1.00							

271

272 **4.2 Comparison of INSAT-3D TPW with Actual Rainfall Observation**

273 The box-whisker plot shown in the Figure 6 compares the actual rainfall observation and INSAT-
274 3D TPW for different values during June to September 2016. This figure is constructed from the
275 daily rainfall observation between 0 to 140 mm occurring over the 34 stations and collocated mean
276 INSAT-3D TPW values between 0 to 90 mm over the entire Indian region. It can be seen from the
277 Figure 6, that TPW is binned for the ranges 0-20, 21-40, 41-60, 61-81 and >80. As seen from the
278 whiskers, the rainfall has least scatter for the 0-20 bin, while for TPW >80 it shows most scatter.
279 The mean and median are almost same for all the TPW bins, except for the TPW >80. There exist
280 exponential behavior between rainfall amounts with higher INSAT-3D TPW values. However,
281 further analysis with more number of observations is required for the quantification of non-
282 linear/exponential relationship. However, atmospheric constituents and synoptic scale of monsoon
283 conditions are an important factor when considering the occurrence of rainfall and satellite derived
284 TPW. It is well demonstrated from the Figure 6, that the heavy and heavy to very heavy rainfall
285 are corresponding to the higher TPW values (60-80 mm and above 80mm). The TPW corresponds
286 to the cloud-free observations and rainfall measurements are for cloudy atmosphere. This can be
287 obviously related to the fact that the heavy rainfall occurs in the presence of higher TPW values
288 (Wu et al., 2003). However, for the light to moderate rainfall amount (less than 40 mm) INSAT-
289 3D TPW is comparable. The moisture convergence, advection of moisture over geographical
290 locations of the subdivisions occasionally receive heavy to very heavy rainfall due to synoptic
291 scale monsoon circulations or its orography. The areas having high orographic region like north
292 eastern parts, Jammu-Kashmir and parts of the Western Ghats (in the west coast of India), have
293 less evaporation and high rainfall as the moisture laden air mass is transported over the regions
294 (Ratnam et al., 2016). Similarly, it is also observed that the rainfall is overestimated in the dry
295 conditions because the falling raindrop evaporates before coming to the surface in dry conditions
296 resulting in the overestimation of rainfall.

297



298

299 **Figure 6. The Box-Whisker plot for comparison of INSAT-3D TPW with actual rainfall**
 300 **over Indian region**

301

302 4.3 Case studies of INSAT-3D TPW with ground base GNSS TPW

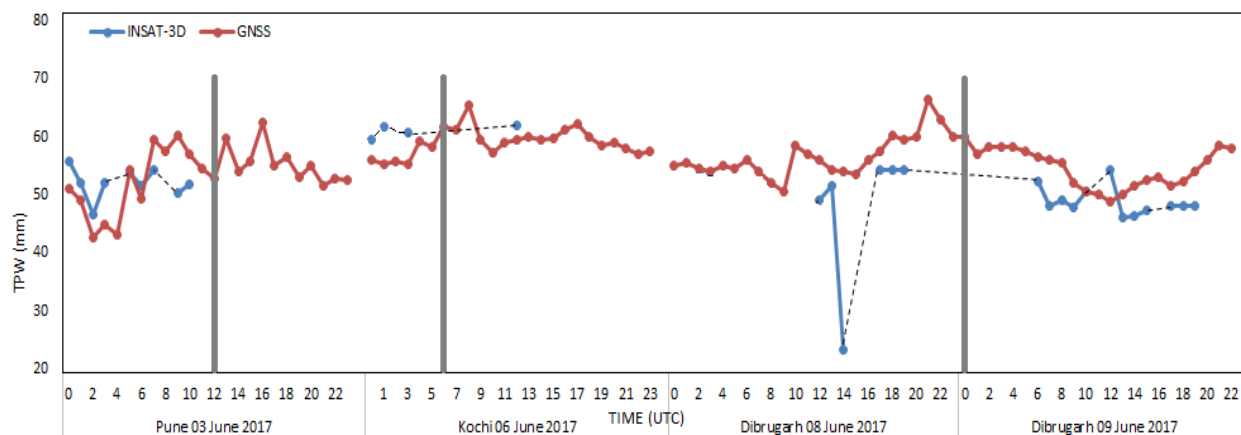
303 In these case studies, hourly INSAT-3D sounder derived TPW, and GNSS TPW were analyzed
 304 for a thunderstorm events occurred in Pune, Kochi and Dibrugarh respectively latitude and
 305 longitude 18.52° E 73.85° N on June 3, 2017 at 1200 UTC, 9.93° E 76.26° N on June 6, 2017 at
 306 0600 UTC and 27.47° E 94.91° N on June 9, 2017 at 0000 UTC. The advantage of GNSS is having
 307 access to multiple satellites, redundancy and availability at all times. Further details can be found
 308 at <http://gnss.imd.gov.in/>.

309 Figure 7 shows the hourly comparison between TPW derived from INSAT and GNSS during
 310 thunderstorm events. The grey bar shows the time of occurrence (i.e., 1200 UTC) of thunderstorm
 311 over Pune city. It was observed from the satellite imageries (not shown here) that initial convection
 312 development starts at 0600 UTC with multiple significant convections. It can be seen from the
 313 Figure 7 that the INSAT-3D TPW is showing the higher TPW values around 53 mm in comparison
 314 with GNSS TPW of 54 mm at 0600 UTC. The higher TPW of INSAT-3D continues up to 1100
 315 UTC which is in agreement with GNSS TPW. The thunderstorm was reported at 1200 UTC. Since
 316 INSAT-3D retrieval cannot be made over cloudy region, the TPW observation was not available
 317 after 1200 UTC.

318 In case of the event at Kochi city, the grey bar shows the time of occurrence at 0600 UTC of
 319 thunderstorm. It was observed from the satellite imageries that initial convection development
 320 starts at 0100 UTC. INSAT-3D TPW is showing the higher TPW values around 58 mm in
 321 comparison with GNSS TPW of 51 mm at 0100 UTC. The TPW observation was not available
 322 after the 0300 UTC due to cloudy conditions. The higher TPW of INSAT-3D continues up to 0300
 323 UTC in agreement with GNSS TPW and thunderstorm was observed at 0600 UTC.

324 At 0000 UTC of thunderstorm over Dibrugarh city was reported. The initial convection
 325 development started at 1800 UTC with values around 53 mm in comparison with GNSS TPW of
 326 58 mm at 1800 UTC. It can be very well seen from Figure 7, there has noted at 1400 UTC with
 327 values 24 mm from 50 mm. This is due to less precipitation occurred in Dibrugarh while 1400 to
 328 1800 UTC, no precipitation has noted due to cloudy sky. The higher TPW of INSAT-3D continues
 329 up to 2000 UTC which is in agreement with GNSS TPW. The thunderstorm was reported at 0000
 330 UTC on June 9, 2017.

331 The case studies show that during the thunderstorm events, INSAT-3D derived TPW compares
 332 reasonably well with GNSS TPW observations, indicating the potential of INSAT-3D derived
 333 TPW for the studies on thunderstorm events. Along with other meteorological parameters (e.g.,
 334 CAPE; convective available potential energy), higher TPW observed during thunderstorm events
 335 can be utilized for studying such events. However, the above case studies confirms the usefulness
 336 of INSAT-3D derived TPW prior to the event and it can be considered as one of the precursors for
 337 mesoscale activity.



338
 339 **Figure 7. A thunderstorm weather event in Pune on 03.06.2017, Kochi on 06.06.2017 and**
 340 **Dibrugarh on 08-09.06.2017**

341

342

5. CONCLUSION

343

344

345

346

347

348

349

350

351

352

353

354

355

356

357

358

359

360

361

362

363

364

365

In the present study, we have assessed the retrieval performance of INSAT 3D derived TPW by comparing it with corresponding observations from RS network and NOAA also GNSS network over the Indian sub-continental. The comparison carried out at daily, monthly and sub-divisional scale covering south Asian monsoon season with different geographical region of the entire Indian sub-continent. The INSAT-3D derived TPW are in good agreement with the TPW derived from *in-situ* measurement (RS) and NOAA satellites. The RMSE and CC found to be around 8 mm and ~ 0.8 in comparison with RS TPW on daily and monthly basis. On sub-divisional scale as a whole, the RMSE and CC against RS and NOAA TPW, found to be 0.80; 0.90 mm and 1.2; 0.91 mm respectively. It is to be noted that the INSAT-3D TPW on monthly scale shown very good agreement with the sub divisional scale rainfall observations. In addition to that, the comparison of INSAT-3D TPW with actual rainfall observation were also made during the same period. It was observed that the heavy and heavy to very heavy rainfall are corresponding well with the higher TPW values. This indicating the reliability to use the TPW product in forecasting advancement of monsoon precipitation over the Indian region. The improvement observed in the current INSAT-3D sounder products TPW is mainly attributed to the GSICS bias corrections applied to the sounder radiances at IMDPS by SAC/ISRO. The advantages of INSAT 3D TPW product offers real time availability over the Indian region with higher spatial (resolution 10 km) and temporal resolution (60 minute) compared to the other derived from polar orbiting satellites. The quality of TPW product of INSAT-3D shows the potential for its usefulness in weather monitoring and forecasting purpose for the improvement in nowcasting over the Indian region. In future study, INSAT-3D and INSAT-3DR derived TPW in staggering mode (every 15-minutes) can be utilized for the detection and the study of mesoscale activity like thunderstorm during pre-monsoon and monsoon season.

366

ACKNOWLEDGMENTS

367

368

369

Authors are grateful to Dr. K. J. Ramesh, the Director General of Meteorology IMD for offering valuable suggestions. We appreciate the work of C. M. Kistawal and P. Thapliyal of applying GSCIS correction at IMDPS for improving sounder retrievals. We thank both them for providing

370 their technical inputs. The first author also thanks NOAA for providing satellite data of TPW used
371 in the comparison against that of INSAT 3D sounder.

372

373

REFERENCES

374 Ackerman, S. A. and G. L. Stephens, 1987: The absorption of solar radiation by cloud droplets:
375 An application of anomalous diffraction theory. *J. Atmos. Sci.*, 44, 1574-1588.

376 Ferraro, R. R., Weng, F., Grody, N. C., Zhao, L., Meng, H., Kongoli, C., Pellegrino, P., Qiu, S.,
377 Dean, S., 2005: NOAA Operational Hydrological Products Derived From the Advanced
378 Microwave Sounding Unit. *IEEE Trans. Geosci. Remote Sens.*, 43, 1036-1049.

379 Hannon, S., Strow, L. L. and Mc Millan, W. W., 1996: “Atmospheric Infrared fast transmittance
380 models: A comparison of two approaches”, *Proc. SPIE – Int. Soc. Opt. Eng.*, 2830, 94-105.

381 Kidder, S.Q. and A.S. Jones, 2007: A blended satellite Total Precipitable Water product for
382 operational forecasting. *Journal of Atmospheric and Oceanic Tech.*, Vol 24, 74-81.

383 Kuo, Y. H., Zou, X. and Guo, Y. R., 1996: “Variational assimilation of precipitable water
384 using a non-hydrostatic mesoscale adjoint model”, *Mon. Wea. Rev.*, 124, 122-147.

385 Kumar, Gajendra, Madan, R., Krishnan, K.C. Sai & Jain, P. K., 2011: Technical and operational
386 characteristics of GPS radiosounding system in upper air network, *MAUSAM*, 62, 3, pg 403-416

387 Li, J. and Huang, H. L., 1999: Retrieval of atmospheric profiles from satellite sounder
388 measurements by use of the discrepancy principle, *Appl. Optics*, 38, 916–923.

389 Li, J., Wolf, W. W., Menzel, W. P., Zhang, W., Huang, H. L., and Ahtor, T. H., 2000: Global
390 soundings of the atmosphere from ATOVS measurements: The algorithm and validation, *J. Appl.*
391 *Meteorol.*, 39, 1248–1268.

392 Ma, X. L., Schmit, T., and Smith, W., 1999: A non-linear physical retrieval algorithm – Its
393 application to the GOES-8/9 sounder, *J. Appl. Meteor.*, 38, 501–503.

394 Mitra, A., Bhan, S., Sharma, A., Kaushik, N., Parihar, S., Mahandru, R., and Kundu, P. K., 2015:
395 INSAT-3D vertical profile retrievals at IMDPS, New Delhi, *Mausam*, 66, 687–694.

396 Ratnam, M. V., Basha, G., Murthy, B. V. Krishna, Jayaraman, A., 2013: Relative humidity
397 distribution from SAPHIR experiment on board Megha-Tropiques satellite mission: Comparison
398 with global radiosonde and other satellite and reanalysis data sets, 118, 1-9.

399 Ratnam, M. V., Kumar, A. H., Jayaraman, A., 2016: Validation of INSAT-3D Sounder data with
400 in-situ measurements and other similar satellite observations over India, *J. Atmospheric*
401 *measurement techniques*, 9, 5735–5745.

402 Schmit T. J., Feltz, W. F., Menzel, W. P., Jung, J., Noel, A. P., Heil, J. N., Nelson, J. P., and Wade,
403 G. S., 2002: Validation and use of GOES Sounder moisture information. *Wea. Forecasting*, 17,
404 139-154.

405 Smith, T. L., Benjamin, S. J., Gutam, S. I., Sahm, S., 2007: Short-Range Forecast Impact from
406 Assimilation of GPS-IPW Observations into the Rapid Update Cycle. *Mon. Wea. Rev.*, 135, 2914-
407 2930.

408 Susskind, J., Barnett, C., Blaisdell, J., Iredell, L., Keita, F., Kouvaris, L., Molnar, G., and Chahine,
409 M., 2006: Accuracy of geophysical parameters derived from Atmospheric Infrared
410 Sounder/Advanced Microwave Sounding Unit as a function of fractional cloud cover, *J. Geophys.*
411 *Res.*, 111, D09S17, doi: 10.1029/2005JD006272.

412 Trenberth, K. E. and Stepaniak, D. P., 2003: Seamless poleward atmospheric energy transports
413 and implications for the Hadley circulation, *J. Climate*, 16, 3706–3722, a.

414 Trenberth, K. E. and Stepaniak, D. K., 2003: Covariability of components of poleward atmospheric
415 energy transports on seasonal and inter annual timescales, *J. Climate*, 16, 3691–3705, b.

416 Trenberth, K. E., Fasullo, J., and Smith, L., 2005: Trends and variability in column-integrated
417 atmospheric water vapor, *Clim. Dyn.*, 24, 741–758.

418 Wu, P., J.-I. Hamada, S. Mori, Y. I. Tauhid, M. D. Yamanaka, and F. Kimura, 2003: Diurnal
419 variation of precipitable water over a mountainous area of Sumatra Island. *J. Appl. Meteorol.*, 42,
420 1107-1115

421 Yuan, L., Anthes, R., Ware, R., Rocken, C., Bonner, W., Bevis, M. and Businger, S., 1993:
422 “Sensing climate change using the global positioning systems”, *J. Geophys. Res.*, 98, 14,925-
423 14, 93.

424

